

BL29XUL: High-resolution Imaging of a Nanostructure Material by Focused X-ray Ptychography

Yukio Takahashi(Osaka Univ., RIKEN) and Nicolas Burdet (RIKEN)

Abstract

Coherent X-ray diffraction imaging (CXDI) is a lensless imaging technique based on coherent diffraction and phase retrieval calculation, which can achieve a high spatial resolution beyond that of conventional X-ray microscopes employing lenses. X-ray ptychography is a method of CXDI for reconstructing extended objects, in which a probe is scanned across the sample and the diffraction pattern is observed at each beam position. The spatial resolution of CXDI is limited, in principle, only by the x-ray wavelength and the largest scattering angle recorded. The use of highly focused incident X-ray beams is effective for collecting high angle diffraction data at a high signal-to-noise ratio. The participants will measure multiple coherent X-ray diffraction pattern from a nanostructure material using high-intense X-rays focused by Kirkpatrick-Baez (KB) mirrors. Finally, we will demonstrate an image reconstruction from the diffraction patterns using phase retrieval calculation. During the practical course the participants will learn how a coherent beam is produced from incoherent radiation, thus how to focus it with KB mirrors and finally how to detect and invert the coherent diffraction radiation to produce a quantitative image of the sample.

Practice

1. Introduction of beamline

The beam line BL29XUL equips a SPring-8 standard in-vacuum undulator, transport channel as long as 1 km and four tandem experimental stations. Figure 1 shows the overall view of BL29XUL. The first experimental hutch (EH1) is placed at 52 m from the source, the second (EH2) is 60.2 m, the third (EH3) is 98 m, and the fourth (EH4) is 987 m. BL29XUL produces X-ray over a wide range of energy range (4.9- 18.7 keV) thanks to both the variable gap of the in-vacuum undulator and the scanning angle of the Si(111) monochromator. The energy resolution is approximately 1.3×10^{-4} . In the practice, we will use 6.500keV monochromatic X-ray beam (wavelength $\lambda = 0.1907$ nm). In EH1, a slit is located, which produces virtual light source. In EH3, KB mirrors, a sample chamber, and CCD are located as shown in Fig. 3. In order to illuminate full coherent X-rays to the KB mirrors, the slit size is adjusted to $10 \times 10 \mu\text{m}^2$. The X-ray beam is transported through the vacuum pipe to EH3.

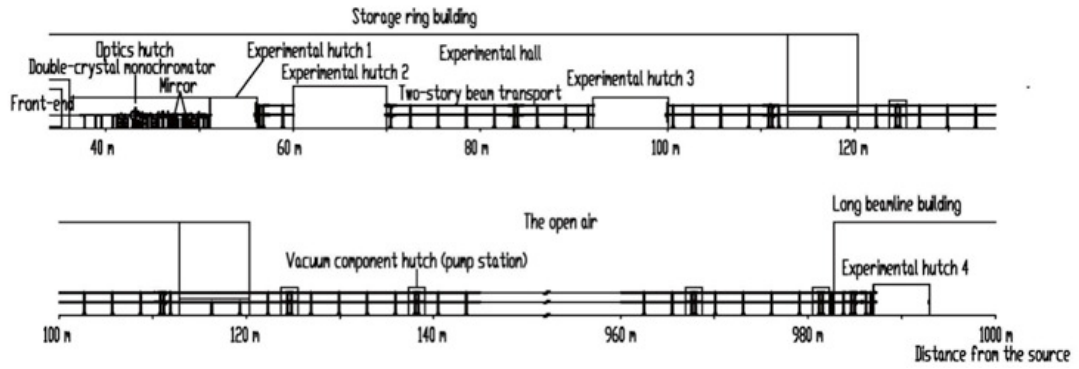


Fig. 1 Overall view of BL29XUL.



Fig. 2 Photograph of apparatus for coherent X-ray diffraction measurements in EH3 of BL29XUL

2. Alignment of the KB mirrors

KB mirrors, which consist of two elliptical mirrors as shown in Fig. 3, are an X-ray focusing device. Table 1 shows a summary of the parameters of the KB mirrors for the practice. The KB mirrors can produce the focused X-ray beam of $\sim 500 \times 500 \text{ nm}^2$ in size at 6.5 keV. In the alignment of the KB mirrors, the glancing angles are precisely adjusted by the combined system of flexure hinges and a linear actuator. The intensity profile on the focal plane is measured by the wire scanning method.

TABLE 1. Parameters of the KB mirrors

	First mirror	Second mirror
Central glancing angle (mrad)	3.5	3.15
Acceptance width (μm)	315	284
Focal length (mm)	1000	895

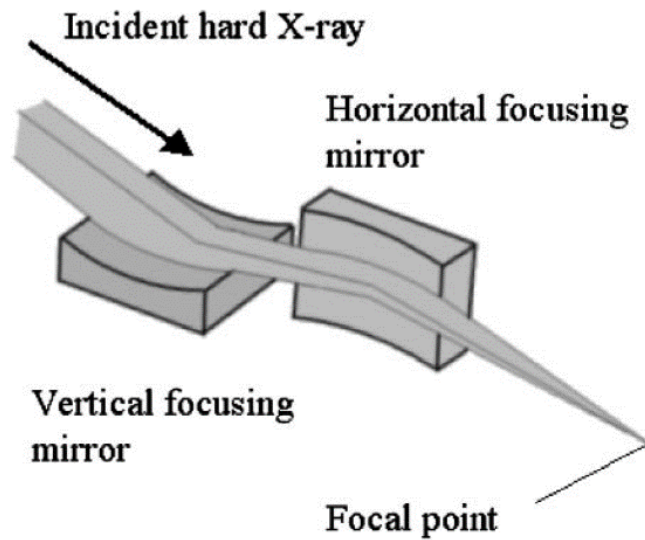


Fig. 3 Schematic illustration of KB mirrors (H. Mimura et al., JJAP **44**, L539-L542 (2005), Fig. 3, ©2005 The Japan Society of Applied Physics)

3. Observation of the sample by optical microscope

The sample is a test object with artificial nanostructures. Figure 4 shows the SEM image of the sample. The 200-nm-thick Pt film is deposited on the 1- μm -thick SiN membrane chip. The SPring-8 logo is fabricated in the Pt film on the membrane using a focused ion beam. In the practice, the test object is observed by optical microscope, in order to measure the distance between the logo and the edge of the window of the membrane.

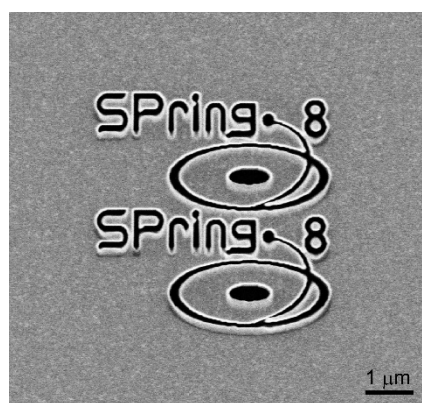


Fig. 4 Scanning electron microscope image of the sample.

4. Measurement of ptychographic diffraction patterns of the sample

The sample is mounted on the stage inside the chamber. By monitoring the X-ray intensities penetrating the sample, the sample is aligned on the focal position. Figure 5 shows the schematic layout of the coherent diffraction pattern measurement of the

sample. The sample is illuminated in 10×10 overlapping fields of view that is spaced by 300 nm. The sample position is precisely controlled by using piezo stages with capacitive sensors. Coherent forward diffraction patterns are recorded using an X-ray direct-detection CCD. The X-ray exposure time at each position is ~ 1 s.

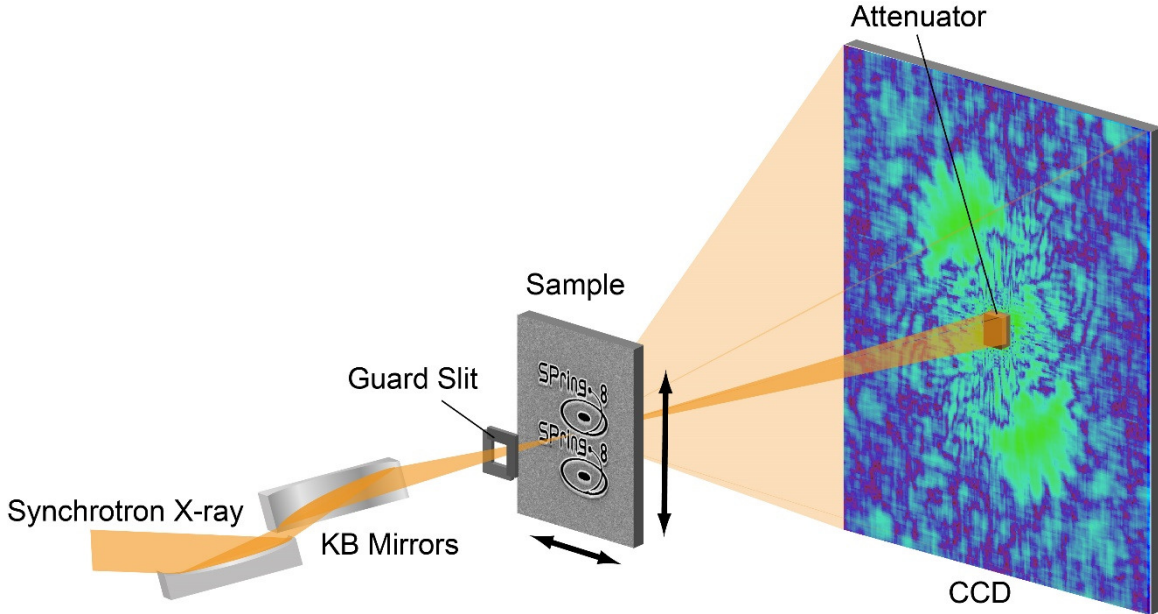


Fig.5 Schematic illustration of focused X-ray ptychography.

5. Data analysis

Finally, we will demonstrate an image reconstruction from the collected diffraction patterns using a phase retrieval algorithm called the Ptychographic Iterative Engine (PIE) which sequentially generates sub-images that agree with the measurements. Its procedure for data analysis is detailed here:

1. A current object transmission function from a shifted position \mathbf{r}_j becomes after multiplication with a localized probe function: $f_j(\mathbf{r}) = o(\mathbf{r} - \mathbf{r}_j)p(\mathbf{r}) = \psi_j$. Then, this complex function evolves (or propagates) to the far field by use of a computational FFT:

$$\Psi_j(\mathbf{q}) = |\Psi_j|e^{(i\phi_j)} = \mathcal{F}[\psi_j(\mathbf{r})]. \quad (1)$$

2. Next, the modulus constraint is applied while preserving the computed phase:

$$\Psi'_j(\mathbf{q}) = \sqrt{I_j}.e^{(i\phi_j)}. \quad (2)$$

3. The inverse Fourier transform of $\mathcal{F}^{-1}[\Psi'_j(\mathbf{q})]$ updates the current view which is in turn used to estimate a new object:

$$o_j^{n+1}(\mathbf{r}) = o_j^n(\mathbf{r}) + \frac{|p(\mathbf{r} + \mathbf{r}_j)|p^*(\mathbf{r} + \mathbf{r}_j)}{|p_{max}(\mathbf{r} + \mathbf{r}_j)||p(\mathbf{r} + \mathbf{r}_j)|^2 + \alpha}. \beta(\psi'_j(\mathbf{r}) - \psi_j(\mathbf{r})). \quad (3)$$

4. The above steps are repeated for each of the j diversity images all over the positions \mathbf{r}_j to update for the object field. Completion is realized after n iterations, with one iteration being interpreted as one pass over all scan positions (The PIE scheme is summarized in Fig. 6).

The overlap constraint between positions implies a multiple update of the different field realizations within a single iteration, and thus dramatically increases the success of converging efficiently to a unique solution. Obviously, the relative strength of the overlapping constrained illumination is the ingredient that favors the convergence of the calculation.

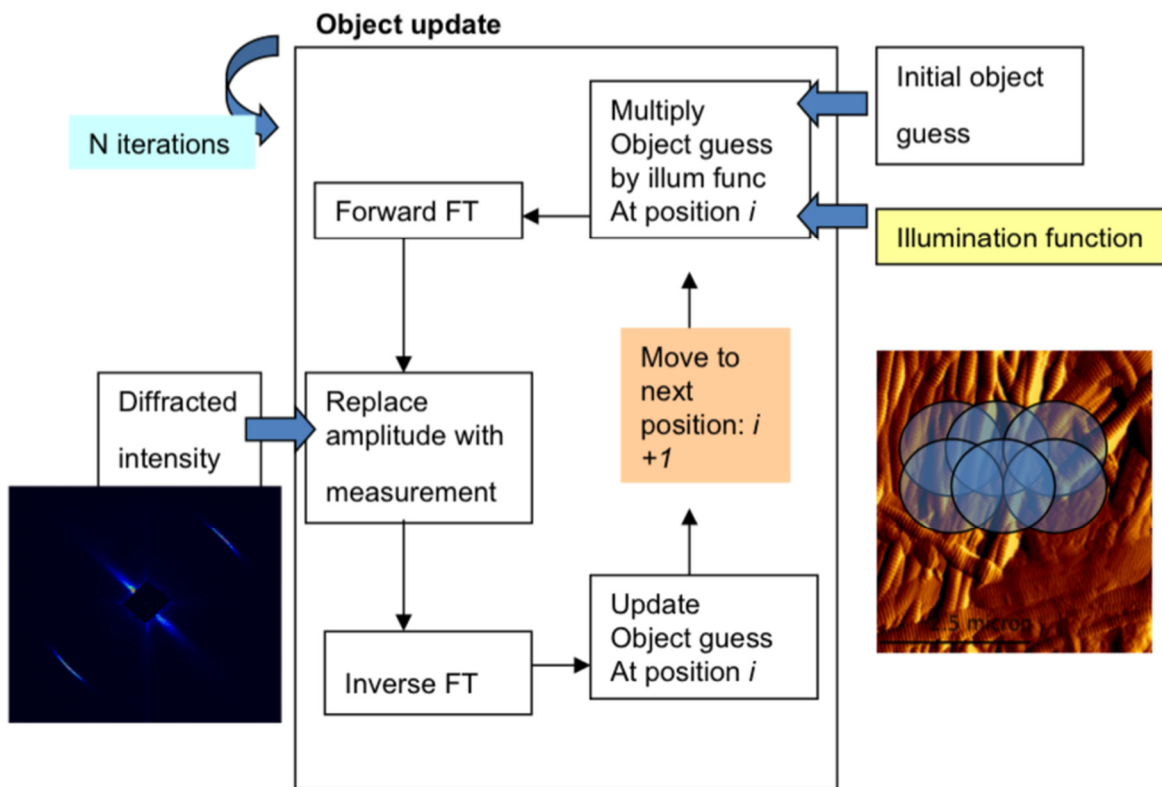


Fig.6 Schematic representation of Ptychographic Iterative Engine.